energies

Article

Design and Analysis of Three Phase Axial Flux Permanent Magnet Machine with Different PM Shapes for Electric Vehicles

Ziaul Islam [1,*], Faisal Khan [1], Basharat Ullah [1,*], Ahmad H. Milyani [2,3] and Abdullah Ahmed Azhari [4]

1 Department of Electrical and Computer Engineering, COMSATS University Islamabad, Abbottabad 22060, Pakistan
2 Department of Electrical and Computer Engineering, King Abdulaziz University, Jeddah 21589, Saudi Arabia
3 Center of Research Excellence in Renewable Energy and Power Systems, King Abdulaziz University, Jeddah 21589, Saudi Arabia
4 The Applied College, King Abdulaziz University, Jeddah 21589, Saudi Arabia
* Correspondence: engr.zia308@gmail.com (Z.I.); basharat.bigb@gmail.com (B.U.)

Abstract: Axial flux permanent magnet (AFPM) machines are good candidates for electric vehicle applications due to their high torque density, improved efficiency, and better flux distribution; thus, they are often used. A dual-rotor single-stator AFPM machine with four differently shaped permanent magnet (PM) rotors is investigated. The main aim of this paper is to enhance the average torque while minimizing the cogging torque and torque ripples at the expense of low PM volume. The proposed machines are analyzed in terms of flux linkage, back-EMF, cogging torque, average torque, and torque ripples. The analysis reveals that the machine with an arc-shaped PM rotor performs better than the others. In addition, the trapozoidal arc-shaped PM used in the AFPM machine outperforms the hexagonal, skew arc, and traditional trapezoidal PMs. The torque density of the trapezoidal-shaped PM machine is 40.23 (KNm/m^3), while that of the hexagonal shape is 32.46 (KNm/m^3), that of the skew arc shape is 39.78 (KNm/m^3), and that of the arc shape is 50.38 (KNm/m^3).

Keywords: axial flux motor; electromagnetic analysis; torque density; 3D FEA

check for updates

Citation: Islam, Z.; Khan, F.; Ullah, B.; Milyani, A.H.; Ahmed Azhari, A. Design and Analysis of Three Phase Axial Flux Permanent Magnet Machine with Different PM Shapes for Electric Vehicles. *Energies* **2022**, *15*, 7533. https://doi.org/10.3390/en15207533

Academic Editor: Frede Blaabjerg

Received: 13 September 2022
Accepted: 8 October 2022
Published: 12 October 2022

1. Introduction

Pollution caused by combustion engines reduces air quality and increases carbon dioxide contamination in the environment, particularly in large cities with high vehicle concentrations. Due to rapid changes in environmental concerns, the phenomenon of hybrid electric vehicles has been focused on as an alternative solution to reduce carbon emissions in transportation [1,2]. The axial flux permanent magnet machine (AFPMM), also known as disc-type motors, is an attractive alternative used for various purposes such as traction application, electric vehicles, hybrid electric vehicles, and aerospace technology; it is also widely used in domestic to industrial and military applications [3,4]. Due to global warming and the rapid changes in carbon abundance, the world has shifted to green energy, which is environmentally friendly. Recently, energy crises in the world have prompted efforts to create "green" alternative forms of transportation, such as electric vehicles with zero emissions driven by batteries or fuel cells, which may unquestionably contribute to the long-term decarburization of road transportation. Therefore, AFPMMs are extensively used worldwide from renewable energy systems to transportation due to their compact structure, light weight, shorter axial length, high filling factor, greater efficiency, and suitable heat removal configuration, and now, they can be considered a mature technology [5,6]. The axial flux PM motor uses an efficient utilization of active material, thus leading the motor to high power and torque density counter to radial motors. Due to its compact structure, the axial motor operates at a lower current density, and the power losses are lower than those of the induction motor [7].

The construction of electrical machines is configured into variously designed shapes, as given in Figure 1. However, there are three main configurations of AFPMMs, i.e., the double-stator single-rotor DSSR also known as a Kaman-type motor, and a double-rotor single-stator DRSS torus motor [8–10]. The double-stator single-rotor machine has complex manufacturability, is less robust, and is challenging in maintenance, which degrades the overall performance of the motor. On the other hand, a single stator double rotor is simple to manufacture, more robust, and easily enhances the overall efficiency of the motor because it has all the desirable characteristics [11]. Moreover, a multi-stage motor consists of more than two rotors and a stator. However, ferrite PM motors are less efficient and have been replaced by rare-earth PM motors, which enhance the motor performance in terms of power density, torque density, and reliability. However, they are also difficult in maintenance and manufacturability [12]. In [13], a study is carried out to analyze the effect of ferrite PM and rare-earth PM on the performance of the AFPMM. There is no winding on the rotor; therefore, a permanent magnet leads the motor to robustness. Toroidal winding is on the stator, which reduces the cost and boosts the performance of the motor with less copper loss and lower weight [14].

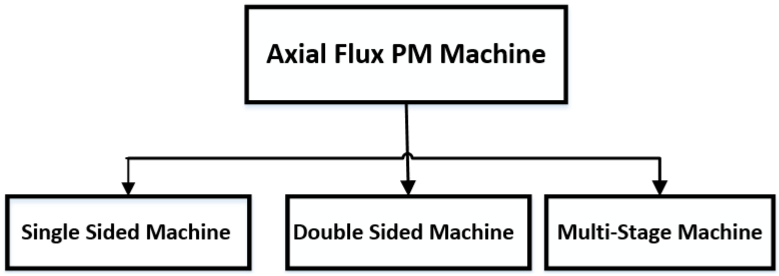

Figure 1. Classification of AFPMMs based on rotor and stator structure.

Significant attention has been given to hybrid electric vehicles, for which synchronous machines are mostly taken into consideration [15]. The use of ferrite PMs is less efficient and unreliable, which are replaced by rare-earth PM. Furthermore, rare-earth PM synchronous machines (PMSMs) are noiseless, durable, easy to maintain throughout their lifetime, much better, and more efficient [16]. PMSMs are classified into radial flux PM (RFPM), axial flux PM (AFPM), and transverse flux PM (TFPM) machines. Counter to the TFPMMs and RFPMMs, the AFPMM machine has a compact structure, smaller volume, and shorter axial length; in addition, it is easy to manufacture, reliable, and durable in maintenance [17]. However, the circulation of flux path in a DSSR Kaman-type motor is complex because it travels through the core of the stator, crosses the air gaps, and enters the core of rotor via the alternate pole (S pole) of the PMs. Moreover, it is not easy for the radial machine to achieve high power density with a slim, thin, and lightweight structure [18]. These incentive features motivated researchers to develop new applications for AFPMMs that are suitable, reliable, durable, and improve their compatibility with the contemporary power market [19].

Axial machines with various topologies are suggested for electric vehicle (EV) applications. Based on a comprehensive electromagnetic investigation, the toroidal winding in the torus axial motor has been found to be the most suitable and durable candidate compared to the yokeless and segmented armature (YASA) motor. The AFPMMs motor with a YASA design shows good performance, but there is an issue of robustness [20]. On the other hand, the torus design has good performance with simple manufacturability and easy maintenance [21]. The flux concentration capability of the torus machine is higher compared to the YASA design. There is not enough cooling system in the YASA design, leading the machine to overheat. An extra cooling system is required, which increases the weight and cost of the motor [22,23]. The stator core of the YASA motor is designed from soft magnetic composite materials, which can reduce manufacturing costs. However, there is an issue of thermal instability, which degrades the efficiency of the motor. The flux path of DSSR is much more complex as compared to a torus motor [24]. On the other hand, the torus motor has a compact structure with easy manufacturability, with an appropriate self-ventilating duct that leads the machine to higher performance [25,26]. Research is carried out on the different types of winding configurations such as concentrated winding, overlap winding, drum winding, closed form solution, and toroidal winding. Compared to these types of windings, toroidal winding has fewer copper losses and shorter end winding, which improves the efficiency and power density of the machine [27]. In a multi-stage motor, the flux path is complicated; the motor also leads to high temperatures and has an inappropriate cooling mechanism that needs an extra cooling system [28,29].

In this context, it has been shown that a specifically designed PM shape can generate sinusoidal back-EMF and significantly reduce torque ripples in AFPMM machines, opening up a new area of research. The designed topology uses an AFPM torus type, i.e., dual-rotor single-stator configuration. The machine has twenty-four coils on the stator, and twenty PMs are housed on the rotor [30]. AFPMM machines suffer from undesirable phenomena such as cogging torque, thermal issues, and demagnetization. A soft magnetic composite (SMC) core is used, which has a low eddy current loss and is an effective solution to improve the performance in terms of thermal issues [31]. Cogging torque is a serious phenomenon that occurs in permanent magnet machines when the stator slot is equal to rotor poles, and the phenomena of cogging torque occurs. As a result of flux fluctuation in the core teeth and rotor magnets, undesirable effects occur such as cogging torque and power losses due to the pulsation of flux in the core teeth and rotor magnets [32]. Different techniques are introduced for the removal of cogging torque, such as skewing, shifting magnets, and pole pairing the magnets. The technique for reducing cogging torque through skewing and shifting is introduced in this study, and up to a certain extent, it successfully achieves the desired target [33,34].

It is essential to increase the torque profile effectively, as this is the most critical demand for electrical machines. It is preferable to maintain the same or lower magnet volume while using various PM shapes to accomplish the required outcomes. As most researchers are attempting to reduce torque ripples while minimizing cogging torque and obtaining higher efficiency at a low expense of PMs, the arc shape machine can endure greater torque capabilities and thus increase the machine's efficiency compared to traditional machines. By reconfiguring the rotor pole number, many forms of rotors, such as arc shape, skewing arc shape, and hexagonal shape are realized. This paper proposed and designed various rotor PM shape designs, magnetizing the PM in the z-direction.

This paper proposes a comparative analysis of a dual-rotor single-stator Torus AFPM motor with different permanent magnet shape designs. A rotor with different permanent magnet shapes is designed. The electromagnetic 3D finite element analysis (FEA) is carried out on all the configured designs. After the electromagnetic analysis, the proposed design DRSS rotor with an arc-shaped PM has better electromagnetic performance in terms of torque and efficiency. The paper is organized as follows: Section 2 introduces the basic design and the operating principle of the proposed AFPM machine. Analysis parameters are discussed in Section 3, while in Section 4, the electromagnetic performance analyses are evaluated. Efficiency calculation is completed in Section 5, and a detailed comparison is made in Section 6, while the conclusion is drawn in Section 7.

2. Design and Working Principle

A three-phase 24-slots and 20-poles (24/20) dual rotor single stator conventional design and proposed designs with different PM shapes are shown in Figure 2. The main machine specifications are listed in Table 1. The suitable PM shape selection process is shown in Figure 3. These designs have the exact stator dimensions and shape; however, the rotor consists of a PM with different shapes, as shown in Figure 4. The stack length, outer, and inner diameter are the main parameters that remained the same. Toroidal winding is used on the stator for more efficient electromagnetic performance, and PM is affixed to the rotor.

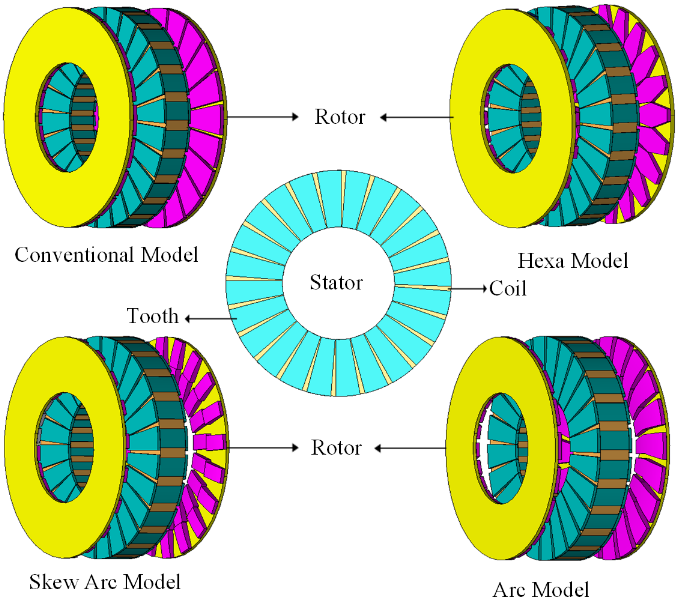

Figure 2. Conventional and proposed AFPMM topologies.

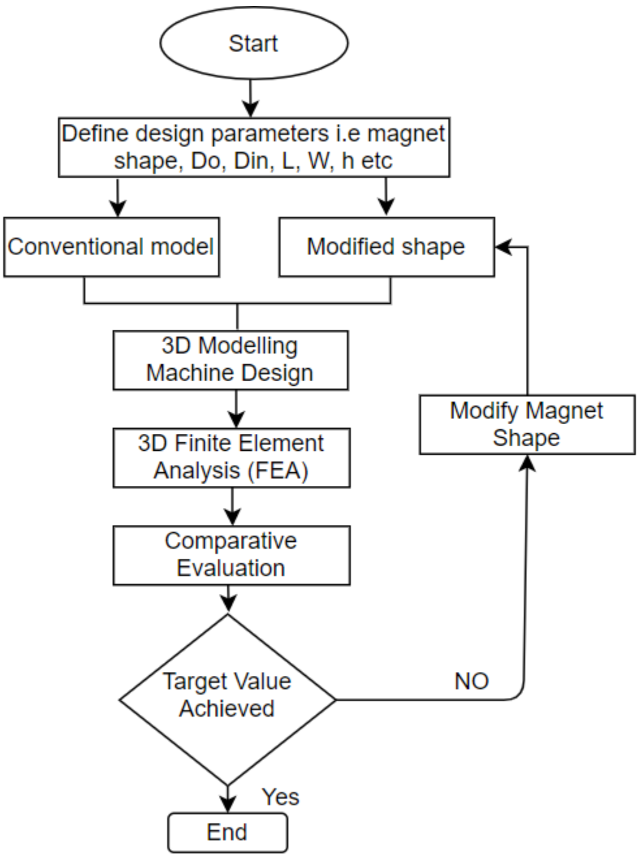

Figure 3. Suitable PM shape selection methodology.

The fundamental working principle is based on the no-load flux of all the proposed machine designs, which is identical to the conventional design. When the three-phase current flows through the stator, the MMF distribution is produced by each set of windings. The flux travels axially because the pole of the magnet on one disc faces the north magnet on the other disc across the airgap and then turns circumferentially and back to the rotor. The average torque produced by the machine is the result of these MMFs interacting with each magnet pole in the rotor. The torus machine is configured with a dual rotor single stator equipped with toroidal winding, which has less end winding and is more efficient. For electromagnetic performance, four different machine designs are carried out. Permanent magnets are placed on the rotor. Counter to the AFPMM, the flux path of the radial machine is relatively larger and more complicated. For achieving higher efficiency, the use of toroidal windings can significantly improve flux-enhancing capability.

Table 1. Geometry parameters of the AFPMM.

Parameter	Value
Axial Length (L)	60 mm
Outer Radius (D_o)	130 mm
Inner Radius (D_{in})	65 mm
Airgap	1 mm
Stator Height (h)	38 mm
Yoke Height	12 mm
Yoke Length	43 mm
PM Height (W)	5 mm
Number of Turns	10
Filling factor	0.75

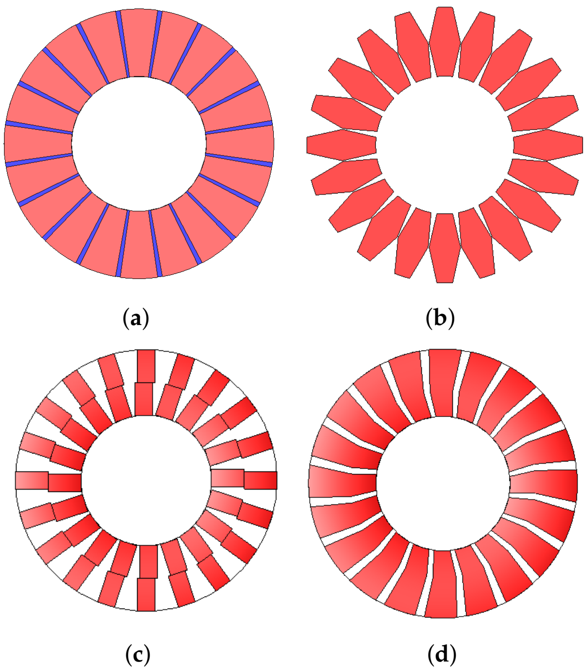

Figure 4. Rotor structure of AFPMM (**a**) conventional rotor (**b**) hexagonal shaped PM (**c**) skew arc shaped PM (**d**) arc shaped PM.

3. Analysis Parameters

All the machines proposed are analyzed on several performance metrics, including their cogging torque (T_{cogg}), torque ripples (T_{rip}), average torque (T_{avg}), and torque density (T_{den}), as well as total harmonic distortion (THD) of all three phases flux linkage. The THD, T_{den} and T_{rip} are found by using Equations (1)–(3), respectively, while the rest of the parameters are obtained from the 3D-FEA solver directly.

$$\text{THD} = \frac{\sqrt{\sum_{i=2}^{m} \Phi_i^2}}{\Phi_1} \times 100\% \tag{1}$$

$$T_{den} = \frac{T_{avg}}{V_m} \tag{2}$$

$$T_{rip} = \frac{T_{max} - T_{min}}{T_{avg}} \quad (3)$$

The flux linkage of the primitive element is denoted by Φ_1, whereas the harmonic components are denoted by Φ_2 to Φ_m. V_m represents the volume of the machine.

4. Electromagnetic Performance Analysis

In this section, the performance parameters, such as flux linkage, cogging torque, back-EMF, average torque, torque, and power vesus speed characteristic curves of the base and proposed designs are evaluated and compared. Figure 5 shows the flux density nephogram of all the designs. JMAG v20.1 is used for the 3D-FEA calculations of all the designs.

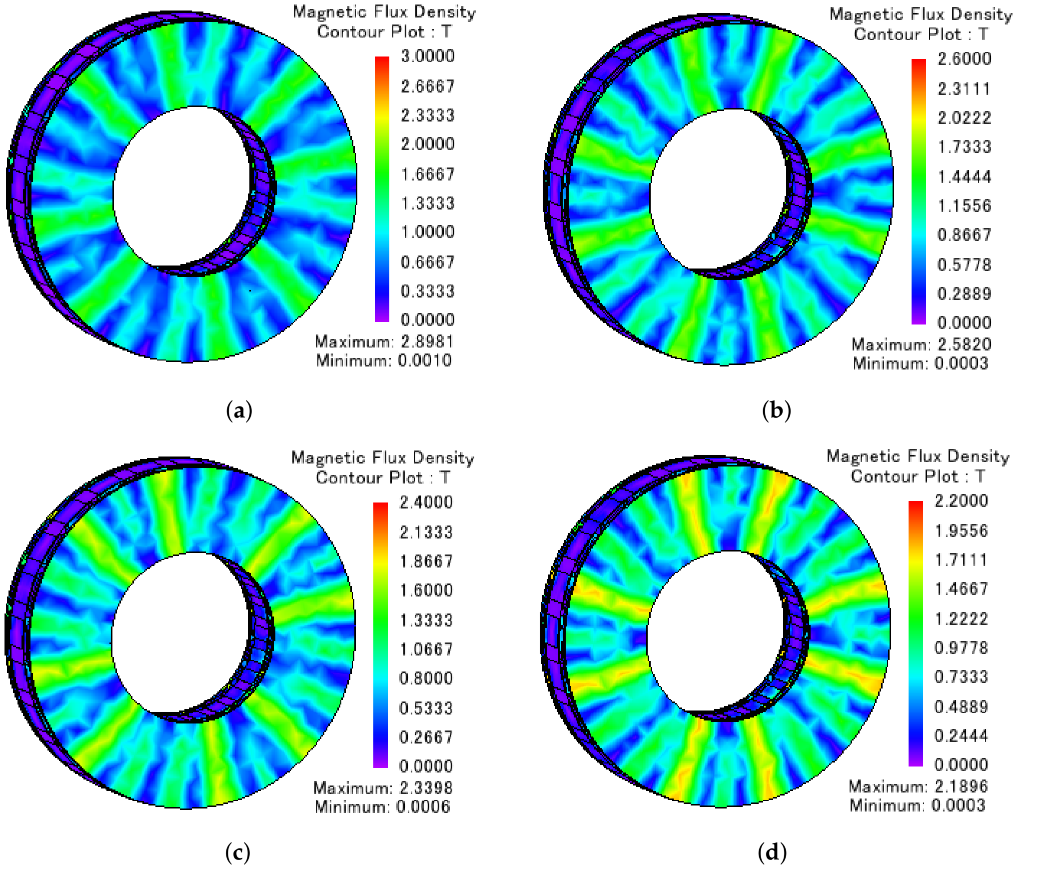

Figure 5. Flux density contour of AFPMM: (**a**) conventional design (**b**) hexagonal-shaped PM design (**c**) skew arc-shaped PM design (**d**) and arc-shaped PM design.

4.1. Flux Linkage

For obtaining a more accurate flux linkage, we have to perform a coil test. In a three-phase machine, there are twenty four coils, and each phase has eight sets of coils. For comparison, a single no-load flux linkage is shown as presented in Figure 6. The THD of the different models are calculated: a conventional model and the proposed skew arc, hexagonal, and arc-shaped PM models. The THD of the base model is 4.42% while the proposed models have 1.66%, 2.68% and 3.06%, respectively. The arc-shaped PM design has better performance than the conventional and the other proposed designs with enhanced flux linkage.

4.2. Back-EMF

When the flux linkage is in a coil change, EMF is induced. The EMF is calculated in Equation (4), and normally, in an electric machine, the T_{avg} is directly related to back-EMF. The flux linkage is represented by (Φ), which is shown in Equation (4). The proposed machines and conventional machine back-EMF are presented in Figure 7 at the executed speed of 1200 r/min. In Figure 8, the THD of the back-EMF for all the designs is shown.

$$\text{Back-EMF} = \frac{d\Phi}{dt} \quad (4)$$

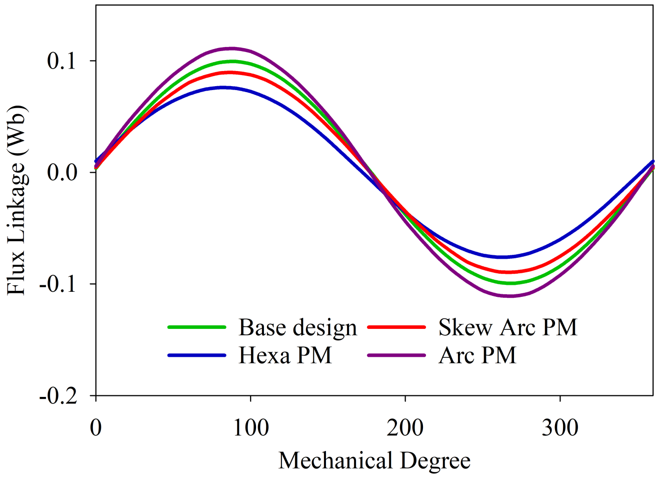

Figure 6. Flux linkage of all the proposed and conventional AFPM machine.

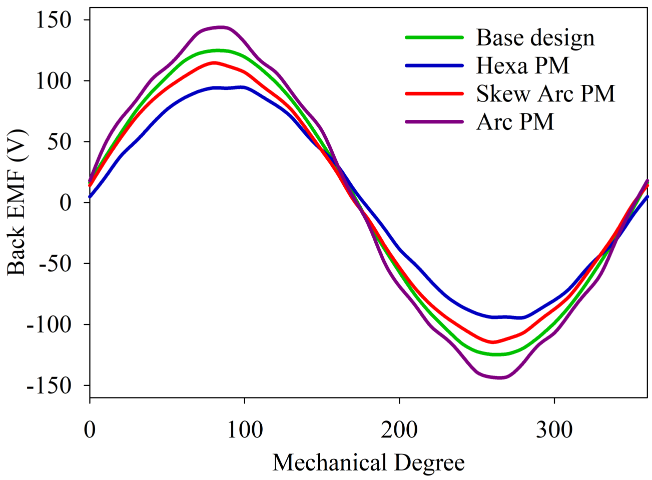

Figure 7. Back-EMF of the proposed and conventional AFPM machine.

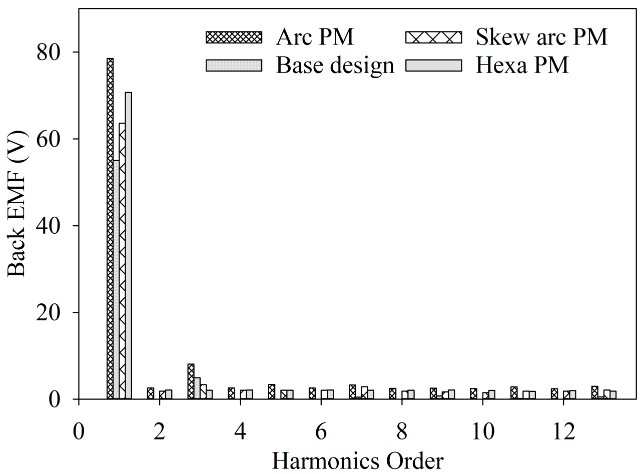

Figure 8. Back-EMF THD of the proposed and conventional AFPM machine.

4.3. Cogging Torque

When the rotor poles are equal to the stator slots, the phenomena of cogging torque occurs. The variation of airgap magnetic energy caused by the interaction of magnetic poles and slotted stators causes cogging torque. The use of PMs in axial machines causes the phenomenon of cogging torque, which arises as a result of the interaction between stator slots and rotor poles. As the electromagnetic torque is the summation of T_{avg} and T_{cogg}, when the cogging torque is higher, the average torque will be lower and vice versa. Moreover, AFPMMs suffer from high cogging torque, which results in noise and vibration. The cogging torque mitigation technique can be applied to the stator and rotor. Additionally, a stiffing and shifting technique is utilized to improve the performance and efficiency of the motor.

For the reduction of cogging torque in an axial flux PM machine, this is the simplest and most efficient method. Many methods have been used to reduce cogging torque, including skewing of the rotor, increasing the number of slots per pole, changing the width slot opening, creating notches on the stator face, distributing the stator slots unevenly, changing the width or length of magnets, changing the magnetic pole magnetization direction, and arranging of rotor poles asymmetrically. Equation (5) is used to compute the cogging torque. Figure 9 shows the cogging torque of the base and three suggested models. Finally, the hexagonal shape machine's cogging torque is lower than that of the other designs.

$$T_{cogg} = -\frac{1}{2}\phi_{gap}^2 \frac{d\phi}{dR} \tag{5}$$

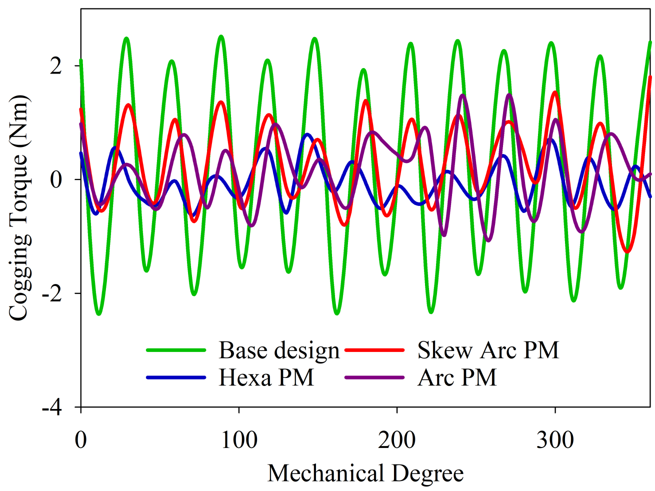

Figure 9. Cogging torque of all the proposed models and the conventional AFPM machine.

4.4. Average Torque

The average torque of a 24-slot/20-poles three-phase machine, including the base and proposed designs, is analyzed and investigated in this section, as shown in Figure 10. The output average torque of the conventional and various proposed models are investigated at a rated current of 6 A/mm^2 and compared. The T_{avg} of the base design is 90.36 Nm, while that of the hexagonal-shaped PM model is 70.79 Nm, that of the skew arc model is 83.61 Nm, and that of the arc-shaped PM model is 101.12 Nm. The proposed design with the arc-shaped PM has the highest average torque.

$$T_{em} = T_{avg} + T_{cogg} \tag{6}$$

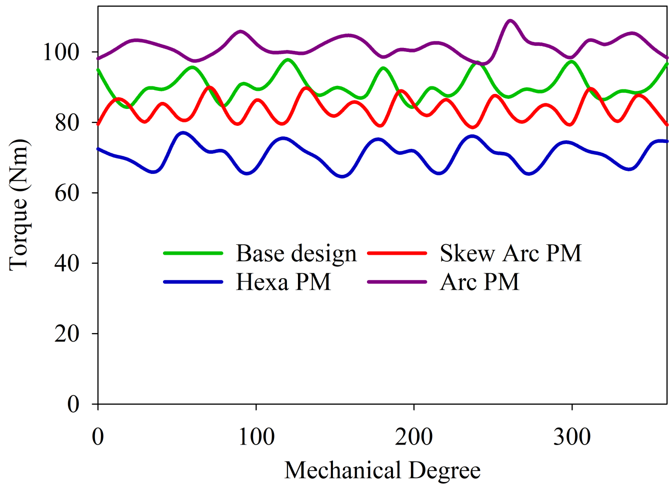

Figure 10. Torque of all the proposed and conventional AFPM machines.

5. Efficiency Calculation

Figure 11 shows the torque vs. speed characteristic curve for the arc-shaped PM design. To calculate machine efficiency, various points on the torque vs. speed characteristic curve are chosen. The performance of the machine is evaluated at various speeds, and the resulting torque is examined as part of the investigation described in the preceding section. The proposed machine's average torque decreases as the speed increases while maintaining constant power at the output. The maximum torque speed curve is defined by these operating points. As shown in Figure 12, the selected operating points are highlighted. In order to calculate efficiency, 3D FEA simulations were run at all operating points, taking into account copper and iron loss. The efficiency can be calculated using Equation (7).

$$\text{Efficiency}(\eta) = \frac{\text{Output Power}}{\text{Output Power} + \text{Losses}} \tag{7}$$

Power vs. Speed Curve

The output power is equal to the product of torque and speed (Equation (8)), which shows that torque and speed are inversely proportional to each other in any machine. Therefore, the torque gradually decreases as the speed of the machine increases to maintain constant power capability. The power of the AFPM machine increases until its rated speed of 3400 rpm. After the rated speed, the proposed machines show constant power capability. Figure 12 shows the power of the AFPM machine at various speeds.

$$P = \tau\omega \tag{8}$$

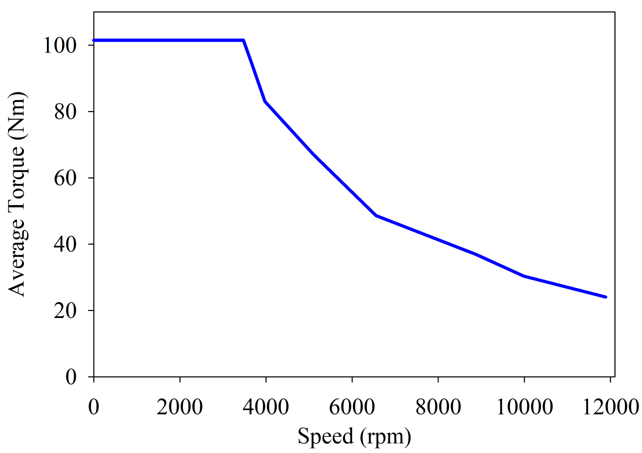

Figure 11. Average torque versus speed characteristic curve of the arc-shaped PM model.

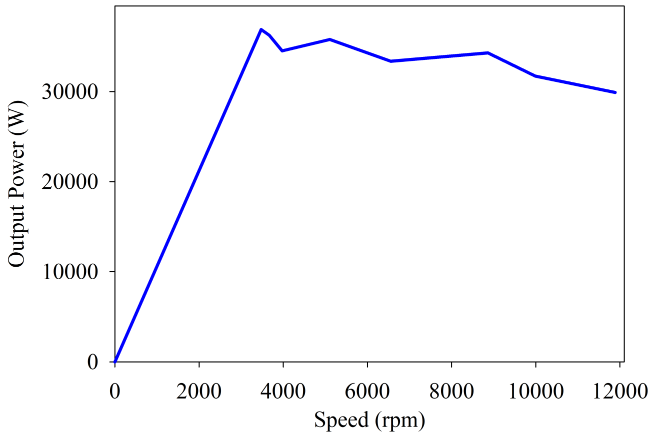

Figure 12. Output power versus speed characteristic curve of the arc-shaped PM model.

The use of finite element analysis (FEA) can quickly and accurately calculate the iron loss of each part of the machine. In this proposed machine, the stator and rotor are made of iron, which is taken into account when calculating the iron losses of the machines by using the 3D FEA. The copper losses are calculated by using Equation (9). Figure 13 shows the number of points taken when the efficiency is calculated. Figure 14 presents the copper losses, iron losses and efficiency of the proposed arc-shaped PM model.

$$P_{cu} = I\rho JL(NQ)(1000) \tag{9}$$

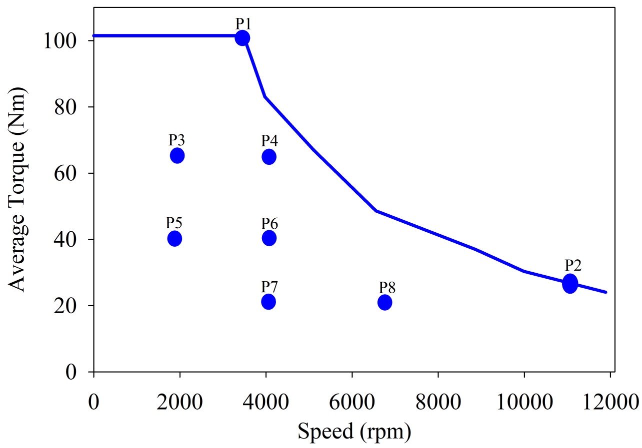

Figure 13. Points at which efficiency is calculated for arc-shaped PM model.

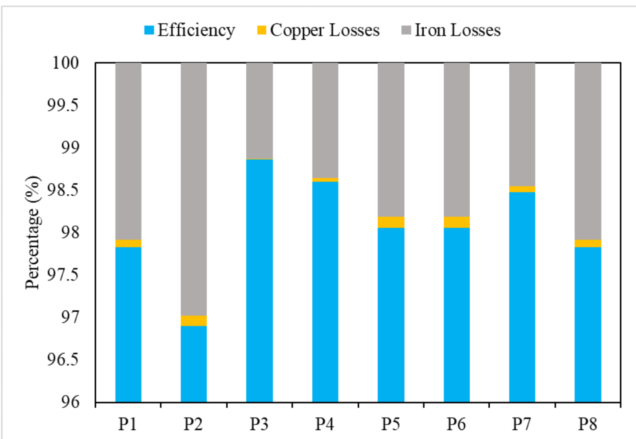

Figure 14. Copper losses, iron losses and efficiency of arc-shaped PM model.

6. Performance Comparison

The performance comparison analysis of the dual-rotor single-stator 24-slots/20-poles AFPM machine with toroidal winding and PM rotors of four different shapes is carried out. The outer/inner diameters, axial length, stator tooth width, air gap length, number of coils turns, slot fill factor, and stator are all kept constant. When compared to a conventional machine, the PM volume of the proposed skew arc model is the same as that of the conventional model, while in the hexagonal and arc models, it is reduced by 21%. The rotor and stator core of the AFPM machine are made of 35H210, whereas the permanent magnets are made of Neomax. Different performance parameters such as no-load flux linkage, back-EMF, THD, torque ripples, and average torque, torque density, power density, and efficiency are analyzed as well. After conducting all of the research analysis, the conventional and three proposed designs with different rotor PM shapes are analyzed; the results are given in Table 2.

Table 2. Quantitative comparison of the proposed and conventional AFPM machine.

Parameters	Base Design	Hexagonal Shaped	Skew Arc Shaped	Arc Shaped
Flux Linkage$_{p\text{-}p}$ (Wb)	0.1165	0.0848	0.1066	0.1322
Flux-THD (%)	4.42	1.67	2.69	3.06
T_{cog} p-p (Nm)	4.72	1.31	2.75	2.45
Back-EMF-THD (%)	17	12	13	9
T_{avg} (Nm)	90.36	70.79	83.61	101.12
T_{rip} (Nm)	4.44	3.63	3.55	6.61
T_{rip} ratio	14.74	15.37	12.73	18.75
T_{den} (kNm/m^3)	40.23	32.46	39.78	50.38
Weight (Kg)	16.90	15.52	16.89	16.35
Power (KW)	32.85	25.74	30.40	36.89
Efficiency (%)	96	84.5	96.5	98.6

7. Conclusions

The design and performance analysis of a three-phase AFPM machine employing a dual rotor single stator with 24 stator slots/20 rotor poles has been investigated. Toroidal winding is used with less end winding and leads the machine to higher performance. The proposed designs with different rotor PMs shapes are analyzed. The conventional and three proposed different rotor machine structures are analyzed and compared. The conventional design has a trapezoidal magnet shape on the rotor, while different proposed PM shapes, i.e., hexagonal, arc, and skew arc shapes, are used in the proposed designs. The electromagnetic performance of these proposed rotors is investigated. The PM volume in the state-of-the-art and skew arc-shaped model is the same, while that in the hexagonal and arc-shaped PM designs is reduced by 21%. In the rotor, for further boosting the efficiency of the machine, a permanent magnet stepping and shifting technique are introduced and employed in a proposed model. The comparative analysis revealed that the proposed arc-shaped model has better electromagnetic performance in terms of coil flux linkage, weight, torque density, and power density with enhanced efficiency. However, the hexa-shaped PM model has lower cogging torque among all the designs.

Author Contributions: Conceptualization, Z.I. and F.K.; methodology, Z.I. and B.U.; software, Z.I. and B.U.; validation, Z.I. and B.U.; resources, F.K., A.H.M. and A.A.A.; formal analysis, B.U., A.H.M. and A.A.A.; original draft preparation, Z.I. and B.U.; visualization, B.U.; review and editing, B.U. and F.K.; supervision, F.K.; project administration, F.K., A.H.M. and A.A.A.; funding acquisition, A.H.M. and A.A.A. All authors have read and agreed to the published version of the manuscript.

Funding: This research received no external funding.

Data Availability Statement: Not applicable.

Conflicts of Interest: The authors declare no conflict of interest.

References

1. Chattopadhyay, R.; Islam, M.S.; Boldea, I.; Husain, I. FEA Characterization of Bi-Axial Excitation Machine for Automotive Traction Applications. In Proceedings of the 2021 IEEE International Electric Machines & Drives Conference (IEMDC), Hartford, CT, USA, 17–20 May 2021; pp. 1–7.
2. Mushid, F.; Dorrell, D. Review of axial flux induction motor for automotive applications. In Proceedings of the 2017 IEEE Workshop on Electrical Machines Design, Control and Diagnosis (WEMDCD), Nottingham, UK, 20–21 April 2017; pp. 146–151.
3. Jussila, H.; Nerg, J.; Pyrhönen, J.; Parviainen, A. Concentrated winding axial flux permanent magnet motor for industrial use. In Proceedings of the XIX International Conference on Electrical Machines-ICEM 2010, Rome, Italy, 6–8 September 2010; pp. 1–5.
4. Kim, J.H.; Li, Y.; Sarlioglu, B. Novel six-slot four-pole axial flux-switching permanent magnet machine for electric vehicle. *IEEE Trans. Transp. Electrif.* **2016**, *3*, 108–117. [CrossRef]
5. Capponi, F.G.; De Donato, G.; Caricchi, F. Recent advances in axial-flux permanent-magnet machine technology. *IEEE Trans. Ind. Appl.* **2012**, *48*, 2190–2205. [CrossRef]
6. Kahourzade, S.; Mahmoudi, A.; Ping, H.W.; Uddin, M.N. A comprehensive review of axial-flux permanent-magnet machines. *Can. J. Electr. Comput. Eng.* **2014**, *37*, 19–33. [CrossRef]
7. Dwivedi, A.; Singh, S.K.; Srivastava, R.K. Analysis and performance evaluation of axial flux permanent magnet motors. *IEEE Trans. Ind. Appl.* **2017**, *54*, 1765–1772. [CrossRef]
8. Zhao, J.; Quan, X.; Sun, X.; Li, J.; Lin, M. Design of a novel axial flux rotor consequent-pole permanent magnet machine. *IEEE Trans. Appl. Supercond.* **2020**, *30*, 1–6. [CrossRef]
9. Capponi, F.G.; De Donato, G.; Rivellini, G.A.; Caricchi, F. Fractional-slot concentrated-winding axial-flux permanent-magnet machine with tooth-wound coils. *IEEE Trans. Ind. Appl.* **2014**, *50*, 2446–2457. [CrossRef]
10. Husain, T.; Tekgun, B.; Sozer, Y.; Hamdan, M. Comparison of axial flux machine performance with different rotor and stator configurations. In Proceedings of the 2017 IEEE International Electric Machines and Drives Conference (IEMDC), Miami, FL, USA, 21–24 May 2017; pp. 1–8.
11. Banchhor, D.K.; Dhabale, A. Design, modeling, and analysis of dual rotor axial flux induction motor. In Proceedings of the 2018 IEEE International Conference on Power Electronics, Drives and Energy Systems (PEDES), Chennai, India, 18–21 December 2018; pp. 1–6.
12. Luk, P.C.K.; Abdulrahem, H.A.; Xia, B. Low-cost high-performance ferrite permanent magnet machines in EV applications: A comprehensive review. *Etransportation* **2020**, *6*, 100080. [CrossRef]
13. Taran, N.; Rallabandi, V.; Ionel, D.M.; Zhou, P.; Thiele, M.; Heins, G. A systematic study on the effects of dimensional and materials tolerances on permanent magnet synchronous machines based on the IEEE Std 1812. *IEEE Trans. Ind. Appl.* **2018**, *55*, 1360–1371. [CrossRef]
14. Si, J.; Zhang, T.; Nie, R.; Gan, C.; Hu, Y. Comparative Study of Dual-Rotor Slotless Axial-Flux Permanent Magnet Machines with Equidirectional Toroidal and Conventional Concentrated Windings. *IEEE Trans. Ind. Electron.* **2022**, *70*, 1216–1228. [CrossRef]
15. Liu, Y.; Zhang, Z.; Wang, C.; Geng, W.; Wang, H. Electromagnetic performance analysis of a new hybrid excitation synchronous machine for electric vehicle applications. *IEEE Trans. Magn.* **2018**, *54*, 1–4. [CrossRef]
16. Usman, A.; Doiphode, N.T.; Rajpurohit, B.S. Stator Winding Faults investigation in Permanent Magnet Synchronous Motor using Motor Signatures: Part I. In Proceedings of the 2019 International Conference on Electrical Drives & Power Electronics (EDPE), The High Tatras, Slovakia, 24–26 September 2019; pp. 160–168.
17. Chowdhury, A.; Das, S.; Tsuda, T.; Saito, N.; Saha, S.; Sozer, Y. Design and Comprehensive Performance Analysis of Transverse Flux and Axial Flux Topologies For Permanent Magnet Synchronous Machines. In Proceedings of the 2021 IEEE Energy Conversion Congress and Exposition (ECCE), Vancouver, BC, Canada, 10–14 October 2021; pp. 3957–3962.
18. Huang, R.; Song, Z.; Zhao, H.; Liu, C. Overview of Axial-Flux Machines and Modeling Methods. *IEEE Trans. Transp. Electrif.* **2022**, *8*, 2118–2132. [CrossRef]
19. Khan, S.; Bukhari, S.S.H.; Ro, J.S. Design and analysis of a 4-kW two-stack coreless axial flux permanent magnet synchronous machine for low-speed applications. *IEEE Access* **2019**, *7*, 173848–173854. [CrossRef]
20. Zhang, B.; Seidler, T.; Dierken, R.; Doppelbauer, M. Development of a yokeless and segmented armature axial flux machine. *IEEE Trans. Ind. Electron.* **2015**, *63*, 2062–2071. [CrossRef]
21. Spooner, E.; Chalmers, B. 'TORUS': A slotless, toroidal-stator, permanent-magnet generator. *IEE Proc. B (Electr. Power Appl.)* **1992**, *139*, 497–506. [CrossRef]
22. Chang, J.; Wang, C. Electromagnetic thermal coupling analysis for a novel cooling system of an axial flux hub motor. *IET Electr. Power Appl.* **2022**, *16*, 421–433. [CrossRef]
23. Li, J.; Lu, Y.; Cho, Y.H.; Qu, R. Design, analysis, and prototyping of a water-cooled axial-flux permanent-magnet machine for large-power direct-driven applications. *IEEE Trans. Ind. Appl.* **2019**, *55*, 3555–3565. [CrossRef]
24. Taqavi, O.; Taghavi, N. Development of a mixed solution of Maxwell's equations and magnetic equivalent circuit for double-sided axial-flux permanent magnet machines. *IEEE Trans. Magn.* **2021**, *57*, 1–11. [CrossRef]
25. Amin, S.; Khan, S.; Bukhari, S.S.H. A comprehensive review on axial flux machines and its applications. In Proceedings of the 2019 2nd International Conference on Computing, Mathematics and Engineering Technologies (iCoMET), Sukkur, Pakistan, 30–31 January 2019; pp. 1–7.

26. Mirzahosseini, R.; Darabi, A.; Assili, M. Magnet shifting for back EMF improvement and torque ripple reduction of a TORUS-type nonslotted axial flux permanent magnet machine. *Int. Trans. Electr. Energy Syst.* **2020**, *30*, e12293. [CrossRef]
27. Muljadi, E.; Butterfield, C.P.; Wan, Y.H. Axial-flux modular permanent-magnet generator with a toroidal winding for wind-turbine applications. *IEEE Trans. Ind. Appl.* **1999**, *35*, 831–836. [CrossRef]
28. Caricchi, F.; Crescimbini, F.; Di Napoli, A. Prototype of innovative wheel direct drive with water-cooled axial-flux PM motor for electric vehicle applications. In Proceedings of the Applied Power Electronics Conference. APEC'96, San Jose, CA, USA, 3–7 March 1996; Volume 2, pp. 764–770.
29. Chang, J.; Fan, Y.; Wu, J.; Zhu, B. A Yokeless and Segmented Armature Axial Flux Machine With Novel Cooling System for In-Wheel Traction Applications. *IEEE Trans. Ind. Electron.* **2020**, *68*, 4131–4140. [CrossRef]
30. Cetin, E.; Daldaban, F. Analyzing the profile effects of the various magnet shapes in axial flux PM motors by means of 3D-FEA. *Electronics* **2018**, *7*, 13. [CrossRef]
31. Li, T.; Zhang, Y.; Liang, Y.; Yang, Y.; Jiao, J. Magnet eddy-current losses reduction of an axial-flux in-wheel motor with amorphous magnet metal. *Int. J. Appl. Electromagn. Mech.* **2021**, *65*, 431–450. [CrossRef]
32. Usman, H.; Ikram, J.; Alimgeer, K.S.; Yousuf, M.; Bukhari, S.S.H.; Ro, J.S. Analysis and optimization of axial flux permanent magnet machine for cogging torque reduction. *Mathematics* **2021**, *9*, 1738. [CrossRef]
33. Cetin, E.; Daldaban, F. Reducing torque ripples of the axial flux PM motors by magnet stepping and shifting. *Eng. Technol. Appl. Sci. Res.* **2018**, *8*, 2385–2388. [CrossRef]
34. Baig, M.A.; Ikram, J.; Iftikhar, A.; Bukhari, S.S.H.; Khan, N.; Ro, J.S. Minimization of cogging torque in axial field flux switching machine using arc shaped triangular magnets. *IEEE Access* **2020**, *8*, 227193–227201. [CrossRef]